Electronic Supplementary Material (ESI) for Sensors & Diagnostics.

SUPPORTING INFORMATION

Genetically engineered filamentous phage for bacterial detection using magnetic resonance imaging

Raymond E. Borg[1#], Harun F. Ozbakir[2#], Binzhi Xu[3#], Eugene Li[2], Xiwen Fang[2], Huan Peng[4], Irene A. Chen*[4], Arnab Mukherjee*[1,2,5,6]

Affiliations:

[1]Department of Chemistry, [2]Department of Chemical Engineering, [3]Biomolecular Science and Engineering, [5]Biological Engineering, [6]Neuroscience Research Institute, University of California, Santa Barbara, CA 93106, USA

[4]Department of Chemical and Biomolecular Engineering, University of California, Los Angeles, CA 90095, USA

*Correspondence should be addressed to IAC (ireneachen@ucla.edu) or AM (arnabm@ucsb.edu)

[#]These authors contributed equally to the work

Methods

Materials and reagents. Zinpyr-1, a fluorescent dye used for assaying free Mn^{2+} was purchased from Adipogen Corporation (San Diego, CA, USA). *Pseudomonas aeruginosa* (Schroeter) Migula cells were purchased from ATCC (Manassas, VA, USA). *Vibrio cholerae* 0395 bacterial cells were a kind gift from Prof. Michael J. Mahan (UC Santa Barbara). *E. coli* Nissle 1917 cells were harvested from a commercial probiotic formulation, Mutaflor®. *E. coli* MG1655 cells were a kind gift from Prof. Charles M. Schroeder (University of Illinois at Urbana-Champaign). Reagents for Gibson assembly and mutagenesis, *E. coli* BL21 strain, and *E. coli* ER2738 strain were purchased from New England Biolabs (Ipswich, MA, USA). Oligonucleotide primers and gBlocks™ were obtained from Integrated DNA Technologies (Coralville, IA, USA). Peptides for the zinpyr-1 based Mn^{2+}-binding assay were synthesized by GenScript (Piscataway, NJ, USA). Reagents for making competent *E. coli* cells were obtained from Zymo Research (Irvine, CA, USA). C57BL/6J mice were purchased from The Jackson Laboratory (Bar Harbor, ME, USA). Sterile hypodermic syringes (16G) were purchased from Air-Tite (North Adams, MA, USA). Depilatory cream was obtained from Reckitt (Parsippany, NJ, USA). Isoflurane and activated charcoal (to scavenge residual isoflurane) were purchased from Akorn Pharmaceuticals (Lake Forest, IL) and Henry Schein (Melville, NY) respectively. All reagents for protein electrophoresis and Western blotting were purchased from Bio-Rad (Hercules, CA, USA). Primary antibody (anti-M13 pVIII #ab9225) was purchased from Abcam (Waltham, MA, USA) and secondary antibody (HRP-conjugated rabbit anti-mouse IgG #61-6520) was purchased from Thermo Fisher (Waltham, MA, USA). All other chemicals and reagents were purchased from MilliporeSigma (St. Louis, MO, USA) or Thermo Fisher Scientific and were of molecular biology grade.

Fluorescence assay for Mn^{2+} binding. A stock solution of $MnCl_2$ (1 mM) was prepared by dissolving the hydrated salt in deionized water. A stock solution of zinpyr-1 (1 mM) was prepared by dissolving the dye in dimethyl sulfoxide (DMSO) and stored in light-tight containers. Stock solutions of full-length (DEHGTAVM) and truncated DP1 peptides (DEHGTA) were prepared in deionized water. Manganese binding assays were performed in 300 µL reaction volumes comprising 4 µM zinpyr-1, 25 µM $MnCl_2$, and peptide concentrations in the range of 0 to 200 µM. The mixture was incubated briefly at room temperature before measuring fluorescence with a

microplate reader (Tecan Spark M200) by exciting zinpyr-1 with blue light (450 nm) and recording the emission spectrum from 485 to 630 nm. The monochromator slit width was set at 20 nm.

Phage plasmid construction and molecular biology. For phage production, we adapted methods previously described in [1,2]. Specifically, phages were produced by sequentially transforming *E. coli* with two plasmids: (1) pPackaging, a helper plasmid that supplies all nine phage packaging proteins and (2) pGFP_Scaf, a phagemid vector containing M13 replication sequences that can be packaged inside the phage capsid (**Figure S2**). The helper plasmid was constructed by modifying the HP17_KO7 plasmid (Addgene #120346) to insert the DP1 coding sequence at the N-terminus of pVIII downstream of the native signal peptide. The phagemid vector was constructed by amplifying the M13 origin of replication from pScaf (Addgene #111401) and subcloning the amplicon using Gibson assembly between the λ T0 and rrnB1 terminator sites in a GFP-expression vector constructed in-house. To design the DP1-CTX phage, a gBlock™ encoding the receptor-binding protein from *V. cholerae* CTXΦ phage was amplified by PCR and sub-cloned (by Gibson assembly) into pPackaging, swapping out the pilus-binding region (amino acids 18-236) of native pIII, but retaining the signaling sequence (amino acids 1-18). All genetic modifications were verified by Sanger sequencing at Genewiz (South Plainfield, NJ, USA) and individual plasmids were propagated by transformation into competent *E. coli* NEB10 cells. Detailed information regarding the key gene sequences is provided in **Table S4**.

Phage purification from *E. coli*. To produce phages, *E. coli* NEB10 cells were first transformed first with the phagemid vector (pGFP_Scaf) and then with the helper plasmid (pPackaging). Doubly transformed colonies were selected on LB-agar plates supplemented with ampicillin (100 µg/mL) and kanamycin (50 µg/mL). A single colony was used to generate a liquid culture by inoculation in 5 mL 2xYT medium (supplemented with kanamycin and ampicillin as before) in a 37 °C orbital shaker (set to 200 r.p.m). The overnight inoculum was sub-cultured at 1:100 dilution (v/v) in 20 mL fresh 2xYT medium (with antibiotics added as above) and grown for another 3-4 hours at 37 °C. This step yielded exponentially growing cells, which were then inoculated in 1 L of fresh LB medium in a 4 L flask and cultured as previously described. After overnight growth, cells were harvested by centrifugation at 7,000 x g for 15 min. The supernatant (~ 0.8 L) was removed and incubated with 0.2 L 5x precipitation buffer (2.5 M NaCl, 20 % PEG-8000 w/v). Following overnight incubation, phages were precipitated by centrifugation of the PEG-treated supernatant at 12,000 x g for 15 min. The supernatant was decanted, and the phage pellet was resuspended in 40 mL HEPES buffer (20 mM, pH 7.0). Cell debris was removed by centrifuging the phage resuspension at 15,000 x g for 15 minutes. The supernatant was mixed one more time with 10 mL of precipitation buffer and chilled on ice for 15-60 minutes before phage particles were precipitated by centrifugation at 12,000 x g for 15 min. The final pellet was resuspended in 10 mL HEPES buffer (20 mM, pH 7.0). All precipitation steps were performed at 4 °C. Phages were verified by Western blotting and phage titer was quantified using absorbance spectroscopy as follows: $phage/mL = \frac{(A_{269} - A_{320})\, x\, (6\, x\, 10^{16})}{\#\ of\ bases\ per\ phage}$ [3]. Here, A_{269} and A_{320} are the absorbance values of the phage suspension at 269 and 320 nm, respectively, and the number of bases was 5153, corresponding to the size of the phagemid vector (pGFP_Scaf). The phages prepared in this manner were stored at 4 °C until use.

Western blotting. Phages were diluted in HEPES buffer (20 mM, pH 7.0) to ~ 24 µM (based on pVIII concentration), mixed 1:1 (v/v) with 2x Laemmli Buffer supplemented with 5% 2-mercaptoethanol, and denatured by heating at 95 °C for 10 min. Approximately 20 µL of the denatured phage was loaded onto a 4-20 % gradient gel (Mini-PROTEAN® TGX Stain-Free gel, Bio-Rad) and separated by electrophoresis at 120 V. Proteins were transferred to a 0.45 µM

PVDF membrane using a Trans-Blot Turbo Transfer System (Bio-Rad). Blocking buffer was prepared by dissolving 5% non-fat dry milk in Tris-buffer saline supplemented with 0.05 % Tween-20 (TBS-T buffer). Antibody dilutions were prepared in blocking buffer at 1:1000 (v/v) for the primary antibody (anti-M13 pVIII) and 1:2000 (v/v) for the secondary antibody (HRP-conjugated rabbit anti-mouse IgG). After the transfer was complete, the PVDF membrane was washed several times with deionized water to remove excess transfer buffer, and subsequently incubated in blocking buffer at room temperature with orbital shaking (200 r.p.m.). After 30 min, the membrane was transferred to primary antibody solution and incubated at 4 °C with gentle shaking (200 r.p.m.). Following overnight incubation, the primary antibody was removed by washing three times with TBS-T, and the membrane was then incubated with a secondary antibody at room temperature for 1 h (200 r.p.m.). Finally, the membrane was washed three times with TBS-T, treated with a chemiluminescent substrate (Clarity Western ECL Substrate, Bio-Rad), and imaged in a gel imager.

Analytical size-exclusion chromatography. PEG-precipitated phage particles (0.5 mL) were injected in a Superdex 200 size exclusion column and washed with at least two column volumes of HEPES buffer at a flowrate of 0.5 mL/min. The elution volume of phage was monitored by inline recording of absorbance at 280 nm.

Inductively coupled plasma mass spectrometry (ICP-MS). ICP-MS experiments were performed using plasticware soaked in 10% nitric acid overnight and rinsed thrice with deionized water. The use of glassware was avoided to prevent contamination due to leaching of impurities from the glass. Mn^{2+}-free and Mn^{2+}-bound phages were dissolved in 5% nitric acid, diluted, and analyzed for Mn^{2+} content using an Agilent 7900 ICP-MS (Agilent Technologies, Santa Clara, CA, USA) at the UC Santa Barbara Bren School of Environmental Science and Management.

Mammalian cell culture and phage treatment. Jurkat and RAW264.7 cell lines were respectively cultured in RPMI and DMEM supplemented with 10 % fetal bovine serum, 100 U/mL penicillin, and 100 µg/mL streptomycin, at 37 ºC, 5 % CO_2 in a humidified chamber. Jurkat cells were grown as suspension cultures, while RAW264.7 cells were grown in adherent format. For phage treatment, RAW264.7 cells were grown till 70-90 % confluency, detached by brief incubation with trypsin-EDTA, and 10 mL of the culture was incubated with phage at approximately the same titer as used for bacterial imaging. Jurkat cells were treated directly with phage, bypassing the trypsin detachment step. Mammalian cells were pelleted by centrifuging at 350 x g for 10 minutes at 4 °C, the lower speeds (compared to bacteria) necessary to prevent cell lysis. The supernatant was decanted and the cell pellet was resuspended in 1 mL HEPES buffer. The wash step was repeated one more time before resuspending the cells in 150 µL HEPES buffer. Finally, the cells were finally centrifuged at 500 x g for 10 min to form pellets, which were imaged using a 7 Tesla vertical-bore MRI scanner exactly as described for bacterial imaging.

For the toxicity assays, a model mammalian cell line (293T) was cultured in DMEM in 6-well plates in supplemented with 10 % fetal bovine serum, 100 U/mL penicillin, and 100 µg/mL streptomycin, at 37 ºC, 5 % CO_2 in a humidified chamber, and incubated overnight with DP1-phage at the same titer as used for the imaging studies. The cells were then detached from the plate by trypsin treatment, resuspended in 1 mL of sterile phosphate buffered saline (PBS), and incubated with 1 mL of 0.4 % trypan blue dye. Non-viable cells retain the blue stain and were identified and counted under brightfield illumination.

Figures & tables

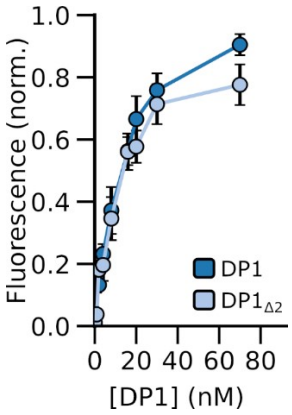

Figure S1. **Fluorescence assay for Mn^{2+} binding to DP1**. Binding was assessed by measuring the fluorescence recovery of quenched zinpyr-1 dye (4 μM), while the full-length or truncated form of DP1 was titrated from 0-70 μM. Fluorescence was recorded by exciting the reaction volume at 450 nm and integrating the emission spectrum from 485 to 630 nm. Values were normalized to peak fluorescence at saturating DP1 (at 8x Mn^{2+} concentration). Error bars represent the standard deviation (n = 3).

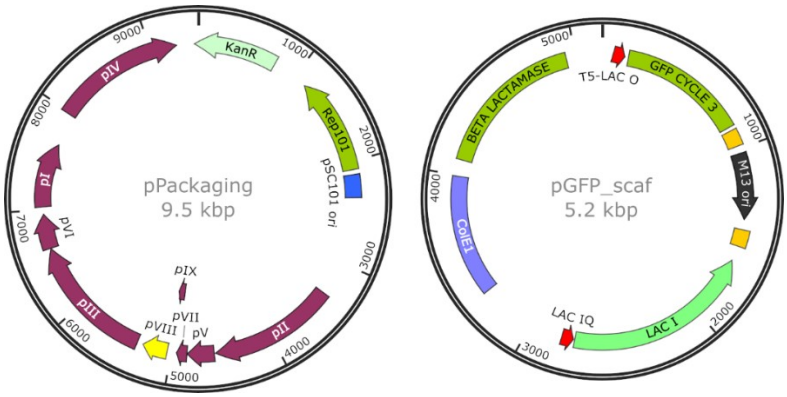

Figure S2. **Modular two-plasmid system for producing DP1-phage**. The pPackaging plasmid encodes all nine proteins required for phage assembly. pVIII (shown in yellow) is modified by inserting the DP1-coding sequence at its 5' end. The pGFP_Scaf plasmid contains the M13 origin of replication and packaging sequences that allow the plasmid to be packaged as a 5153 nucleotide long circular single-stranded (css) DNA ensheathed by the phage capsid.

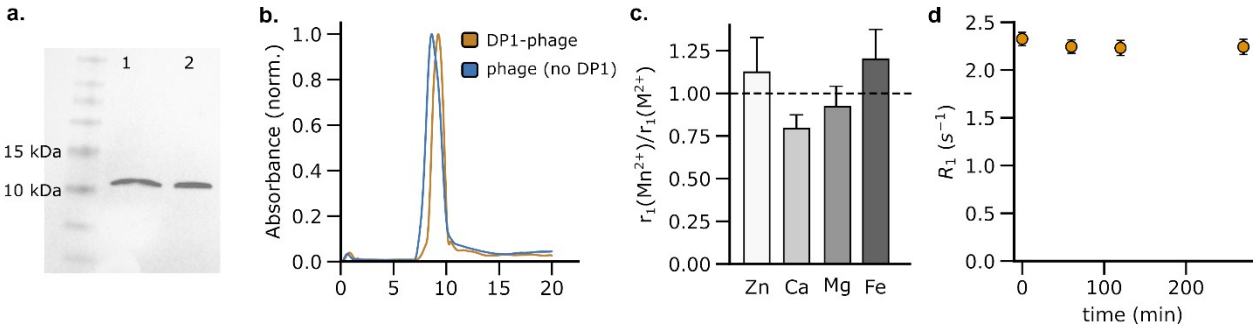

Figure S3. **Biochemical characterization of DP1-phage**. **(a)** Formation of DP1-phage (lane 2) was verified by Western blotting using an antibody targeting pVIII. Lane 1 contains an identically purified M13 phage lacking DP1. **(b)** Phage formation was assayed using analytical size-exclusion chromatography. DP1-phage was found to elute at nearly the same volume as M13 phage lacking DP1. **(c)** Specificity of DP1-phage towards Mn^{2+} was assessed by measuring phage relaxivity (r_1) following incubation of Mn^{2+}-loaded DP1-phage with other divalent metal ions (M^{2+}) supplemented at biologically relevant extracellular concentrations: 10 uM (Zn^{2+}), 1.8 mM (Ca^{2+}), 1 mM (Mg^{2+}), and 20 μM ($FeSO_4$). No significant fold-change in r_1 was detected under these conditions (two-tailed *t*-test *P*-value > 0.6, n = 3-4). **(d)** To test the stability of phage-bound Mn^{2+} ions, the relaxation rate (R_1) of Mn^{2+}-loaded phage was measured for 4.5 hours at 7 T. Zn^{2+} (75 μM) was added as a potentially competing divalent species. No significant change in R_1 was detected under these conditions (two-tailed *t*-test *P*-value > 0.2 at all time points, *n* = 3).

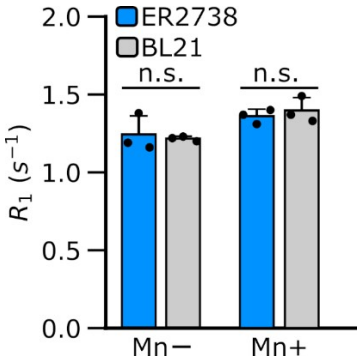

Figure S4. Mn^{2+} alone does not produce strain-specific relaxation enhancement in *E. coli*. Incubation of *E. coli* ER2738 (F-positive) and BL21 (F-negative) strains with $MnCl_2$ produced a modest increase in their spin-lattice relaxation rates ($\Delta R_1/R_1$ = 12.3 ± 0.6 % for ER2738 and 11.8 ± 0.2 % for BL21) but the enhancement was statistically indistinguishable between the two strain types (two-tailed *t*-test *P*-value = 0.18, n = 3). Error bars represent the standard deviation.

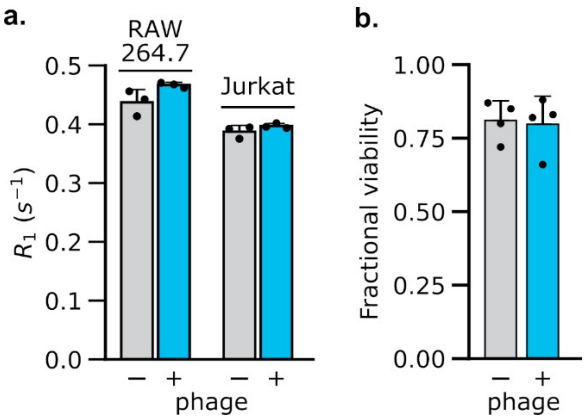

Figure S5. Effect of DP1-phage on mammalian cells. **(a)** Spin-lattice relaxation rates (R_1) of representative mammalian cell lines: Jurkat and RAW264.7, did not show a significant change following incubation with Mn^{2+}-labeled DP1-phage (two-tailed *t*-test *P*-value > 0.5, *n* = 3). **(b)** Phage treatment did not cause toxicity in a representative mammalian cell line (293T) as the viable cell fraction did not change significantly following treatment with Mn^{2+}-loaded DP1-phage for 24 hours. Viability was assessed by measuring trypan blue uptake in 269 phage-free and 360 phage-treated cells in n = 4 non-overlapping fields of view (2-sided *t*-test *P*-value > 0.8). Error bars represent the standard deviation.). Error bars represent the standard deviation.

Table S1. Current MRI probes for bacterial detection

Contrast agent	Targeting	Limitations	*In vivo* application
Gd-DOTA [4]	Zn(II) dipicolylamine	limited specificity: targets anionic groups in the cell membrane	
Gd-DOTA [5]	neomycin	limited specificity: targets gram positive bacteria, relies on antibiotics	bacteria labeled *ex vivo* & injected in the flank
Gd-DOTA (Li et al., 2021)	vancomycin	limited specificity: targets gram positive bacteria, relies on antibiotics	probe injected locally at infection site in the flank
Gd_2O_3 [6]	maltodextrin	limited specificity: maltodextrin is internalized by bacteria broadly	
Magnetic graphitic nanocapsules [7]	boronic acid	limited specificity: targets peptidoglycan in cell wall, generates negative contrast (T_2-weighted)	probe delivered orally to the GI tract
Iron oxide nanoparticles [8]	none	non-specific, generates negative contrast (T_2-weighted)	bacteria labeled *ex vivo* & injected in the flank, footpad

Table S2. Phage-based (non-MRI) probes for bacterial imaging in deep tissues

Probe	Modality	Targeting	Limitations
Single-walled nanotubes bound to a 8-residue peptide displayed on pVIII [9]	near infrared	native pIII to target *E. coli* (F^+), antibody conjugated to pIII to target *S. aureus*	limited depth penetration, low spatial resolution
Chemically conjugated Alexa750 [10]	near infrared	same as above	limited depth penetration, low spatial resolution
Chemically conjugated ^{99m}Tc [11]	nuclear imaging	native pIII to target *E. coli* (F^+) strains	needs ionizing radiation, low spatial resolution

Table S3. Phage-based MRI probes for tumor imaging

Contrast agent	Targeting	Potential limitations
Iron oxide nanoparticles bound to Glu_3 displayed on pVIII [12]	SPARC-binding peptide fused to pIII to target tumors	Generates negative contrast
Iron oxide nanoparticles covalently linked to the phage coat [13]	A synthetic peptide fused to pIII to target apoptotic cells	Generates negative contrast
^{129}Xe-binding cage (cryptophane) covalently attached to pVIII [14]	Antibody fused to pIII to target HER2 receptors in cancer cells	Relies on hyperpolarized ^{129}Xe imaging, which is less commonplace than T_1/T_2 MRI

Table S4. Genetic constructs engineered/used in this work

Construct	DNA sequence (5′ to 3′)
Signal peptide-**DP1**-pVIII	atgaaaaagtctttagccctcaaagcctctgtagccgttgctaccctcgttcc gatgctgtctttcgctgatgaacatggcaccgcggtgatggctgagggtgacg atcccgcaaaagcggcctttaactccctgcaagcctcagcgaccgaatatatc ggttatgcgtgggcgatggttgttgtcattgtcggcgcaactatcggtatcaa gctgtttaagaaattcacctcgaaagcaagctga

Signal peptide-**CTX**-pIII	gtgaaaaaattattattcgcaattcctttagttgttcctttctattctcactc cgccccatcggtaacggcttccgccatcaattgtgatcctaatactactacgt cacaccagttacttttcggttttggctctcccattgtgcaatcggtgttattt gatggctgcatgcttgatattgaaaaagatgactatggttttgtttggtcttg tctctcaaatgaaaatggggactattgcaaggggctctacaaaccccgttttt cacaaggggtatccccgaactggccgatgtgcgacttgtccggagcatctgca gagcgctgcatttatccttattgccctgaggggggaagagtgcgttcccttacc accttcaccgcccagtgattcccctgttgatgggctgagcagctcgtttaagt ctgcgttcaatcaggtctataaaaaccaatcagagatggcttcgactctcaat catgtcagtggtcaggtgtcccactctcaagatatggttcagctcaatacgaa gtttcacgcggatcgtgttcttgagagtgtcaccgcagtcaacaatcgtttgg gtgggcaaatggagtatcttgaggaaatccgcattgatgtttgggatacgcaa cgggaggtaagaaaagccaaggatgagctttactctcgtgttgcggctgtttc atacgatgtgctttatagcgagcttaatgtccttcgggcgattgatgaactta aagactcactcggtgggactgtcgttgctggcggcggctctggtggtggttct ggtggcggctctgagggtggtggctctgagggtggcggttctgagggtggcgg ctctgagggaggcggttccggtggtggctctggttccggtgattttgattatg aaaagatggcaaacgctaataaggggggctatgaccgaaaatgccgatgaaaac gcgctacagtctgacgctaaaggcaaacttgattctgtcgctactgattacgg tgctgctatcgatggtttcattggtgacgtttccggccttgctaatggtaatg gtgctactggtgattttgctggctctaattcccaaatggctcaagtcggtgac ggtgataattcacctttaatgaataatttccgtcaatatttaccttccctccc tcaatcggttgaatgtcgccctttttgtctttggcgctggtaaaccatatgaat tttctattgattgtgacaaaataaacttattccgtggtgtctttgcgtttctt ttatatgttgccacctttatgtatgtattttctacgtttgctaacatactgcg taataaggagtcttaa
M13 origin of replication	acgcgccctgtagcggcgcattaagcgcggcgggtgtggtggttacgcgcagc gtgaccgctacacttgccagcgccctagcgcccgctcctttcgctttcttccc ttcctttctcgccacgttcgccggctttccccgtcaagctctaaatcgggggc tccctttagggttccgatttagtgctttacggcacctcgaccccaaaaaactt gatttgggtgatggttcacgtagtgggccatcgccctgatagacggtttttcg ccctttgacgttggagtccacgttctttaatagtggactcttgttccaaactg gaacaacactcaaccctatctcgggctattcttttgatttataagggattttg ccgatttcgg

References

1. P. M. Nafisi, T. Aksel and S. M. Douglas, *Synthetic Biology*, 2018, **3**, ysy015.
2. U. Tsedev, C.-W. Lin, G. T. Hess, J. N. Sarkaria, F. C. Lam and A. M. Belcher, *ACS Nano*, 2022, **16**, 11676–11691.
3. L. A. Day and R. L. Wiseman, *Cold Spring Harbor Monograph Archive*, 1978, **8**, 605–625.
4. L. M. Matosziuk, A. S. Harney, K. W. MacRenaris and T. J. Meade, *European Journal of Inorganic Chemistry*, 2012, **2012**, 2099–2107.
5. L. Zhang, Y. Liu, Q. Zhang, T. Li, M. Yang, Q. Yao, X. Xie and H.-Y. Hu, *Anal. Chem.*, 2018, **90**, 1934–1940.
6. C. Xu, Z. Li, O. U. Akakuru, C. Pan, R. Zou, J. Zheng and A. Wu, *ACS Appl. Bio Mater.*, 2021, **4**, 3762–3772.

7. Y. Li, X. Hu, D. Ding, Y. Zou, Y. Xu, X. Wang, Y. Zhang, L. Chen, Z. Chen and W. Tan, *Nat Commun*, 2017, **8**, 15653.

8. V. Hoerr, L. Tuchscherr, J. Hüve, N. Nippe, K. Loser, N. Glyvuk, Y. Tsytsyura, M. Holtkamp, C. Sunderkötter, U. Karst, J. Klingauf, G. Peters, B. Löffler and C. Faber, *BMC Biol*, 2013, **11**, 63.

9. N. M. Bardhan, D. Ghosh and A. M. Belcher, *Nat Commun*, 2014, **5**, 4918.

10. N. M. Bardhan, D. Ghosh and A. M. Belcher, *J Biophotonics*, 2014, **7**, 617–623.

11. M. Rusckowski, S. Gupta, G. Liu, S. Dou and D. J. Hnatowich, *Journal of Nuclear Medicine*, 2004, **45**, 1201–1208.

12. D. Ghosh, Y. Lee, S. Thomas, A. G. Kohli, D. S. Yun, A. M. Belcher and K. A. Kelly, *Nature Nanotech*, 2012, **7**, 677–682.

13. J. Segers, C. Laumonier, C. Burtea, S. Laurent, L. Vander Elst and R. N. Muller, *Bioconjugate Chem.*, 2007, **18**, 1251–1258.

14. K. K. Palaniappan, R. M. Ramirez, V. S. Bajaj, D. E. Wemmer, A. Pines and M. B. Francis, *Angewandte Chemie International Edition*, 2013, **52**, 4849–4853.